Exclusive Development of T cell Neoplasms in Mice Transplanted with Bone Marrow Expressing Activated *Notch* Alleles

By Warren S. Pear,* Jon C. Aster,‡ Martin L. Scott,* Robert P. Hasserjian,‡ Benny Soffer,* Jeffrey Sklar,‡ and David Baltimore*

*From the *Department of Biology, Massachusetts Institute of Technology, Cambridge, Massachusetts 02139; and the ‡Department of Pathology, Brigham and Women's Hospital, Harvard Medical School, Boston, Massachusetts 02115*

Summary

Notch is a highly conserved transmembrane protein that is involved in cell fate decisions and is found in organisms ranging from *Drosophila* to humans. A human homologue of Notch, *TAN1*, was initially identified at the chromosomal breakpoint of a subset of T-cell lymphoblastic leukemias/lymphomas containing a t(7;9) chromosomal translocation; however, its role in oncogenesis has been unclear. Using a bone marrow reconstitution assay with cells containing retrovirally transduced *TAN1* alleles, we analyzed the oncogenic potential of both nuclear and extranuclear forms of truncated TAN1 in hematopoietic cells. Although the Moloney leukemia virus long terminal repeat drives expression in most hematopoietic cell types, retroviruses encoding either form of the TAN1 protein induced clonal leukemias of exclusively immature T cell phenotypes in ~50% of transplanted animals. All tumors overexpressed truncated TAN1 of the size and subcellular localization predicted from the structure of the gene. These results show that TAN1 is an oncoprotein and suggest that truncation and overexpression are important determinants of transforming activity. Moreover, the murine tumors caused by TAN1 in the bone marrow transplant model are very similar to the TAN1-associated human tumors and suggest that TAN1 may be specifically oncotropic for T cells.

The human *TAN1* gene encodes a transmembrane protein (TAN1) that contains an extracellular domain possessing a series of motifs, among which are iterated epidermal growth factor (EGF)[1]–like repeats, Notch/lin-12 repeats, and a pair of evolutionarily conserved cysteine residues; the intracellular portion contains ankyrin-like repeats, a glutamine-rich region, and a PEST sequence (Fig. 1) (1). Each of these motifs is also found in the protein product of *Notch*, a *Drosophila melanogaster* gene that appears to control cell fate decisions among equipotent progenitor cells in the developing fly (2, 3). TAN1 is expressed at relatively high levels in developing and adult thymus, suggesting that it might participate in normal T cell development (1, 3a).

TAN1 was originally identified through analysis of the (7;9)(q34;q34.3) chromosomal translocation found in a subset of acute human T cell lymphoblastic leukemias/lymphomas (T-ALL) (1, 4). This rearrangement fuses the 3′ portion of *TAN1* on chromosome 9 to the TCR-β locus on chromosome 7. The resulting allele is deleted for most of the coding sequence of the extracellular domain of TAN1. It directs the synthesis of a series of truncated polypeptides of ~100–125 kD that have NH_2-termini lying near the transmembrane domain (Aster. J., R. Hasserjian, F. Davi, and J. Sklar, manuscript submitted for publication). The t(7;9)-specific polypeptides localize predominantly to the nucleus, probably because of two conserved nuclear localization sequences within the cytoplasmic domain of TAN1 (Aster, J., et. al., manuscript submitted for publication). Nuclear TAN1 has not been detected in cell lines expressing normal TAN1 transcripts or in developing murine thymus (3a), raising the possibility that altered subcellular localization might influence transforming activity.

Although analysis of three tumors bearing the t(7;9) showed consistent disruption of the *TAN1* gene at the chromosomal breakpoint at almost identical positions within the gene (1), the contribution of altered TAN1 to transforma-

[1]*Abbreviations used in this paper:* EGF, epidermal growth factor; FSC, forward scatter; 5-FU, 5-fluorouracil; LTR, long terminal repeat; MoMLV, Moloney murine leukemia virus; RIPA, radioimmunoprecipitation assay; SSC, side scatter; SCF, stem cell factor; Su(H), Suppressor of Hairless; T-ALL, T cell lymphoblastic leukemia/lymphoma; WBC, white blood cell.

 J. Exp. Med. © The Rockefeller University Press • 0022-1007/96/05/2283/09 $2.00
Volume 183 May 1996 2283–2291

tion is unknown. One of the three tumors studied, SUP-T1, had lost both normal *TAN1* alleles, suggesting that *TAN1* might be a tumor suppressor gene (1, 5). Alternatively, removal of the extracellular domain of the protein by the translocation might cause constitutive activity of the intracellular domain, producing a dominant oncoprotein. The latter possibility is supported by the results of mutational analysis in *Drosophila* in which deletions removing the extracellular domain of *Notch* have been shown to lead to dominant gain-of-function phenotypes, opposite to those produced by loss-of-function mutations associated with inactivation of the gene (6–8).

To examine whether TAN1 can function as an oncoprotein, we have used recombinant retroviruses to express, in vivo, proteins resembling the truncated polypeptides found in cells bearing t(7;9). Tumors developed in ~50% of mice that received bone marrow transduced by 5′ deleted forms of *TAN1*. In all cases, the tumors were T cell neoplasms of an immature phenotype. Expression of either cytoplasmic or nuclear forms of TAN1 resulted in a nearly identical disease. This suggests that transformation by TAN1 results primarily from overexpression and truncation of the protein, rather than subcellular localization. These results also directly implicate TAN1 in the pathogenesis of t(7;9) human T-ALL.

Materials and Methods

Retroviral Vectors and Constructs. ΔECT^+ and ΔECT^- were constructed by ligating JK5T, a previously described *TAN1* cDNA (1), to a PCR product spanning base pairs −14 to +70, which encodes the 5′ *TAN1* translational start site and signal peptide. Each construct was subcloned into the BclI site of the pGD retroviral vector (9). The mature polypeptides encoded by ΔECT^+ and ΔECT^- are predicted to be composed of amino acids 1673–2555 and 1704–2555 and to have NH_2-termini located 61 and 30 amino acids external to the transmembrane domain, respectively. ICT was constructed by ligating an oligonucleotide containing an ATG translational start site to a unique Bsu36I site within the JK5T cDNA. The resultant construct encodes amino acids 1770–2555 and is predicted to produce a polypeptide consisting of the entire intracellular region of TAN1 minus the first 13 amino acids. Sequencing of the 3′ long terminal repeat (LTR) of pGD has shown that it is derived from the Moloney murine leukemia virus (MoMLV) LTR (M. Scott, unpublished data).

Retroviral Production and Bone Marrow Infection Protocols. Transfection of the retroviral vectors, cocultivation with 5-fluorouracil (5-FU)-treated bone marrow, and injection into lethally irradiated BALB/cByJ recipients were performed as previously described (10). Cocultivation of the transfected Bosc23 cells and 5-FU-treated bone marrow was performed in a cocktail consisting of DME, 10% heat-inactivated FBS (JRH Biosciences, Lenexa, KS), 5% WEHI-conditioned medium, 6 U/ml recombinant mouse IL-3 (Genzyme Corp., Cambridge, MA), 10,000 U/ml recombinant mouse IL-6 (Genzyme), 5U/ml recombinant mouse stem cell factor (SCF) (Genzyme), 1 μg/ml polybrene (Sigma Chemical Co., St. Louis, MO), 100 U/ml streptomycin (GIBCO BRL, Gaithersburg, MD), 100 U/ml penicillin (GIBCO BRL), and 2 mM L-glutamine (GIBCO BRL). Between 5×10^5 and 1×10^6 nonadherent cells were injected into a tail vein of each recipient animal. Bone marrow and spleen cells from all tumors were cultured in DME supplemented with 20% heat-inactivated FBS (JRH Biosciences), 100 U/ml streptomycin (GIBCO BRL), 100 U/ml penicillin (GIBCO BRL), 2 mM L-glutamine (GIBCO BRL), and 4 U/ml recombinant mouse IL-2 (Genzyme). Bone marrow cells derived from mice T6, I8, and I22 adapted to continuous in vitro growth. Tumor cells from all ΔECT animals were readily transplantable to syngeneic mice. Transfer of ICT tumors to secondary recipients was not attempted. BALB/cByJ mice were obtained from Jackson Laboratories (Bar Harbor, ME) and maintained at the animal facilities at Rockefeller University and Massachusetts Institute of Technology under specific pathogen-free conditions.

Protein Analysis and Immunohistochemistry. Radioimmunoprecipitation assay (RIPA) extracts (11) were prepared from cell lines and tumors, and 10 μg of protein was subjected to electrophoresis in 6% discontinuous SDS–polyacrylamide gels and then transferred electrophoretically to nitrocellulose membranes. The blot was probed with affinity-purified polyclonal rabbit anti-TAN1 raised against the T3 region of the cytoplasmic domain (Fig. 1) and developed by a chemiluminescent method (Amersham International, Little Chalfont, Buckinghamshire, UK). DNA encoding a portion of *TAN1* termed T3 (codons 1733–1877) was amplified by PCR from JK5T (1), ligated into the vector pGEX-4T (Pharmacia), and subsequently purified from detergent lysates with glutathione–Sepharose beads (Pharmacia Biotech, Inc., Piscataway, NJ) (11). Serum from immunized rabbits was affinity purified by sequential passage over an AffiGel-15-GST column (Bio-Rad Laboratories, Hercules, CA) and an AffiGel 15-GST-T3 column. For immunohistochemistry, sections cut from paraffin-embedded tissue were deparaffinized and boiled in a 5% urea solution for 10 min (12). Immunoperoxidase staining was performed with affinity-purified rabbit anti-T3 according to a previously described method (13). Slides were counterstained with hematoxylin. For staining of T6E and I22 cells, the cells were allowed to adhere to poly-L-lysine–coated slides, fixed in 3% paraformaldehyde, and permeabilized with 0.1% saponin. Indirect immunofluorescent and immunoperoxidase staining was performed with affinity-purified anti-T3 and secondary anti–rabbit antibody linked to FITC (Sigma) or HRP (Sigma), respectively.

Flow Cytometry. Spleen cells or LN cells were obtained from mice T8A1, I8, T3A2, T7, or age-matched controls and analyzed for forward scatter (FSC), side scatter (SSC), and expression of Thy1.2, CD4, and CD8 by multiparameter flow cytometry as described (14). For each animal, FACS® analysis was performed on tumor samples derived from at least two different sites, and in all cases, results from the different sites were concordant (data not shown). Control spleen was obtained from an age-matched BALB/cByJ mouse. T8A1 spleen cells were derived from a mouse that had received 10^5 T8 tumor cells, and T3A2 LN cells were derived from a mouse that had received 10^5 T3 bone marrow cells. The staining patterns of the primary T8 and T3 tumors were very similar to the patterns found in T8A1 and T3A2. Antibodies used were the following: CD8a-FITC (YTS169.4; Caltag Laboratories, San Francisco, CA), CD4-PE (YTS191.1; Caltag), TCRβ-PE (H57-597; Caltag), TCRγ/δ-PE (GL3; Caltag), Thy1.2-FITC (5a-8; Caltag), CD3-FITC (500-A2; Caltag), B220-PE (RA3-6B2; Caltag), MAC-1-PE (M1/70.15; Caltag), and CD24-PE (M1/69; PharMingen, San Diego, CA). Fluorescence was analyzed on a FACScan® flow cytometer with CellQuest software (Becton Dickinson, San Jose, CA).

DNA Analysis. High molecular weight DNA was isolated from fresh or snap-frozen tissues, digested with appropriate re-

striction enzymes, and analyzed by Southern blot hybridization as previously described (10). For each animal, DNA was prepared from tumors from at least two different sites. In each case, the proviral integration patterns were identical in the tissues from multiple sites (data not shown).

Results

Retroviral Expression of Truncated TAN1 in Murine Bone Marrow Induces T-cell Neoplasms. To assess the transforming potential of truncated TAN1 in hematopoietic cells, three *TAN1* cDNA constructs (Fig. 1) were cloned into the pGD retroviral vector (9). This retroviral vector expresses the truncated *TAN1* gene under the control of the promoter elements of the MoMLV LTR. Two constructs, ΔECT^+ and ΔECT^-, encoded polypeptides consisting of the TAN1 signal peptide fused to sequences just external to the transmembrane domain. The major difference between these two polypeptides was that one retained a pair of evolutionarily conserved extracellular cysteines (ΔECT^+), whereas the other did not (ΔECT^-). Both of these constructs produced polypeptides that localized predominantly to endoplasmic reticulum and nuclear membrane when stably overexpressed in NIH 3T3 cells (Aster, J., unpublished data). The third construct, ICT, encoded most of the cytoplasmic domain of TAN1 and showed predominantly nuclear localization when transiently or stably overexpressed in murine fibroblasts (Aster, J., unpublished data). These forms were chosen for three reasons. First, the size of the encoded polypeptides (~120 kD for the ΔECT polypeptides and ~110 kD for ICT) roughly resembles that of the polypeptides found in cells bearing the t(7;9). Second, the different subcellular localization of the encoded polypeptides serves to test the importance of nuclear localization in transformation. Finally, comparison of ΔECT^+ and ΔECT^- might identify a role for the conserved extracellular cysteine residues in transformation, a possibility suggested by the observation that mutation of either of these two residues in Notch produced a gain-of-function phenotype in the fly (8).

These *TAN1* constructs were individually transfected into the ecotropic retroviral packaging line, Bosc23, and the resulting high titer retroviral supernatants were used to infect BALB/cByJ bone marrow in vitro (10). 10 lethally irradiated syngeneic mice received bone marrow infected with each construct. From 11 to 40 wk after transplant, 11 mice showed sudden onset cachexia and increases in their white blood cell (WBC) counts coincident with the appearance of leukemic blasts in the peripheral blood. One additional mouse, T3, became cachectic and had circulating blasts without increased WBCs (Table 1). Tumors arose in four mice receiving ΔECT^+ bone marrow, in three mice receiving ΔECT^- marrow, and in five mice receiving ICT marrow, suggesting that the tumorigenicity of each construct was approximately equivalent. This suggests that the presence or absence of the conserved extracellular pair of cysteine residues does not influence transforming activity. The observed frequency with which tumors arose (30–50%) is probably less than the actual frequency, as several sudden and unwitnessed deaths occurred in each group.

At necropsy, five of the mice had thymic masses, while seven mice contained only thymic remnants, the latter being consistent with postirradiation involution (Table 1). 10 of 12 mice had lymphadenopathy and marked hepatosplenomegaly secondary to extensive infiltration and distortion by leukemic blasts (not shown). The remaining two animals, T3 and I9, had microscopic leukemic cell infiltration of spleen and liver.

TAN1-associated Tumors are Composed of Immature T cells. Flow cytometric analysis showed that each of the 12 tumors was composed of immature T cells (Fig. 2). While all 12 tumors reacted with antibodies to Thy1.2 (Fig. 2 and data not shown) and TCR-β chain (not shown), individual tumors showed variable patterns of reactivity with anti-

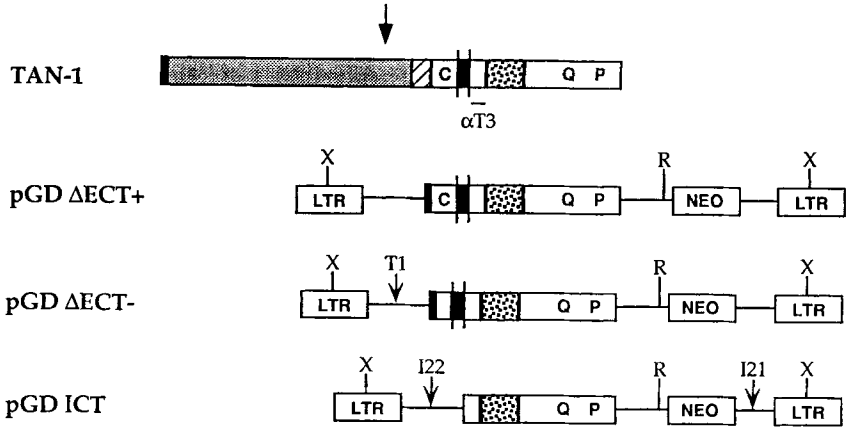

Figure 1. Structure of *TAN1* and ΔECT and ICT cDNA constructs used in the bone marrow transplant experiments. The arrow indicates the approximate site at which the *TAN1* cDNA sequence is disrupted by recombination of *TAN1* with *TCR-β* in tumors with t(7;9) (q34; q34.3) (1). The deletion in T1 occurred 5′ to the cDNA insert in the pGD vector and is indicated by T1. The deletion in I21 occurred 3′ to the cDNA insert in the pGD vector and is indicated by I21 and the deletion in I22 occurred 5′ to the cDNA insert in the pGD vector and is indicated by I22. The T3 region of TAN1 used for immunization is underlined. Legend: black, hydrophobic leader; stippled, EGF-like repeats; diagonally striped, LNR repeats; C- paired, conserved cysteines residues located 49 and 42 amino acids external to the transmembrane domain; black but with extended lines, transmembrane domain; dotted, ankyrin repeats; *Q*, glutamine-rich region; *P*, PEST sequence; *X*, XbaI; *R*, EcoRI. The MoMLV LTR and *neo* resistance gene of the pGD retroviral vector are indicated.

Table 1. *Summary of Tumors in TAN1 Transplants*

Animal	Construct	Latency (weeks)	Terminal WBC/mm^3	Thymic involvement
T1	ΔECT−	11	70	No
T3	ΔECT−	16	4	No
T4	ΔECT−	12	68	No
T6	ΔECT+	15	42	Yes
T7	ΔECT+	40	65	Yes
T8	ΔECT+	15	41	No
T14	ΔECT+	16	55	Yes
I8	ICT	25	25	Yes
I9	ICT	25	32	No
I21	ICT	18	40	No
I22	ICT	18	50	No
I46	ICT	21	150	Yes

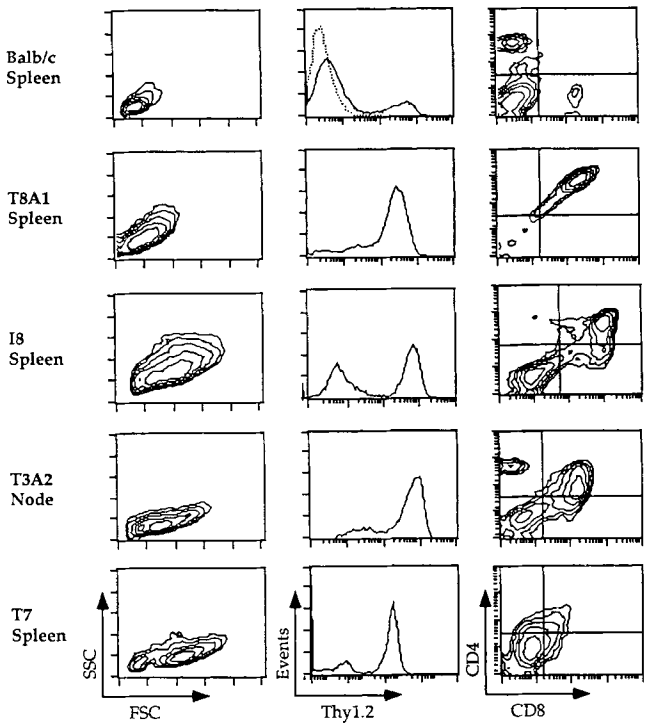

Figure 2. Immunophenotyping of TAN1-associated tumors by flow cytometry. Two-parameter contour plots show FSC versus SSC (*left*) and CD4 versus CD8 expression (*right*). Cursors on the right were set on the basis of profiles of normal splenocytes and thymocytes. A single-parameter histogram shows the expression of Thy1.2 (*solid lines, center column*). The dotted line in the upper panel shows Thy1.2 expression in unstained control spleen cells. The tumors were negative for macrophage (Mac-1) and B-cell (B220) markers, as well as for expression of TCR-γ/δ. In all tumors, the majority of cells expressed TCR-α/β and low levels of CD3.

CD4 and anti-CD8. The observed immunophenotypes revealed cell populations ranging from predominantly Thy1.2$^+$ CD4$^-$ CD8$^-$ double negative cells (Fig. 2, T7), resembling immature cortical thymocytes, to predominantly Thy1.2$^+$ CD4$^+$ CD8$^+$ double positive cells (Fig. 2, T8A1 and I8, and also T1, T4, I9, and I46 [not shown]), resembling a more mature cortical thymocytic phenotype. Five tumors (T3, T6, T14, I21, and I22) expressed high levels of CD8 and lower levels of CD4 (Fig. 2, T3A2 and data not shown), compatible with a maturation stage between double-negative and double-positive cells (15, 16). Additional studies showed that cell lines derived from several of these tumors (T6, I8, and I22) had intermediate to high level surface expression of CD24 (heat stable antigen) and expressed RAG-2 (Pear, W., unpublished data), features also shared by normal cortical thymocytes (17, 18). RAG-2 expression was also observed in liver infiltrated by the T3 and T7 tumors (Pear, W., unpublished data). As exemplified by I8 and T3A2 (Fig. 2), some tumors contained several subpopulations of cells with distinct immunophenotypes.

TAN1-induced Tumors Contain Integrated Proviruses and Overexpress Truncated Forms of TAN1. All tumors contained integrated proviruses, as shown by Southern (DNA) blot analysis (Figs. 3 *a* and 4 *a*). The proviral structure was intact in nine tumors, while three contained small deletions that mapped within vector sequences flanking the cDNA inserts (see Fig. 1). Further blot analysis showed that 10 of 11 tumors that could be evaluated contained a single integrated provirus, while one tumor, T3, contained two unique proviral sequences (Figs. 3 *b*, 4 *b*, and data not shown). Clonal TCR Jβ2 rearrangements were observed in 9 of 11 tumors evaluated (Figs. 3 *c* and 4 *c*). Because tumor infiltration in the spleen and liver of the I9 mouse was minimal, this tumor could not be evaluated for proviral integration number or TCR-β rearrangement.

All of the tumors expressed the introduced truncated forms of TAN1 at high levels relative to the levels of endogenous murine TAN1 (Notch1) in normal BALB/cByJ thymus, spleen, and liver, and the T cell line AKR (Figs. 5 *a* and 5 *b*, and data not shown). BALB/c thymus contained a protein of ~120 kD (p120) (Fig. 5 *a*) that is derived from full-length TAN1 by proteolytic cleavage at a site just external to the transmembrane domain (Aster, J., et al., manuscript submitted for publication). p120 is closely related in primary structure to both the t(7;9)-specific polypeptides and the ΔECT-encoded polypeptides. It is also overexpressed by tissue culture cells transduced by a retrovirus carrying a full-length *TAN1* cDNA, indicating that full-length TAN1 serves as a precursor molecule for p120 (19, Aster, J. et al., submitted). Despite its structural resemblance to oncogenic forms of truncated TAN1, p120 does not appear to be oncogenic, since none of 10 mice receiving bone marrow infected with a retrovirus expressing full-length TAN1 developed TAN1-expressing tumors over the course of 1 yr (Pear, W., and J. Aster, unpublished data).

Both Cytoplasmic and Nuclear Forms of TAN1 Are Oncogenic. Microscopic examination of pathologically enlarged spleen, liver, and LNs showed infiltration by leukemic blasts (Fig. 6 *a*, and data not shown). Immunohistochemis-

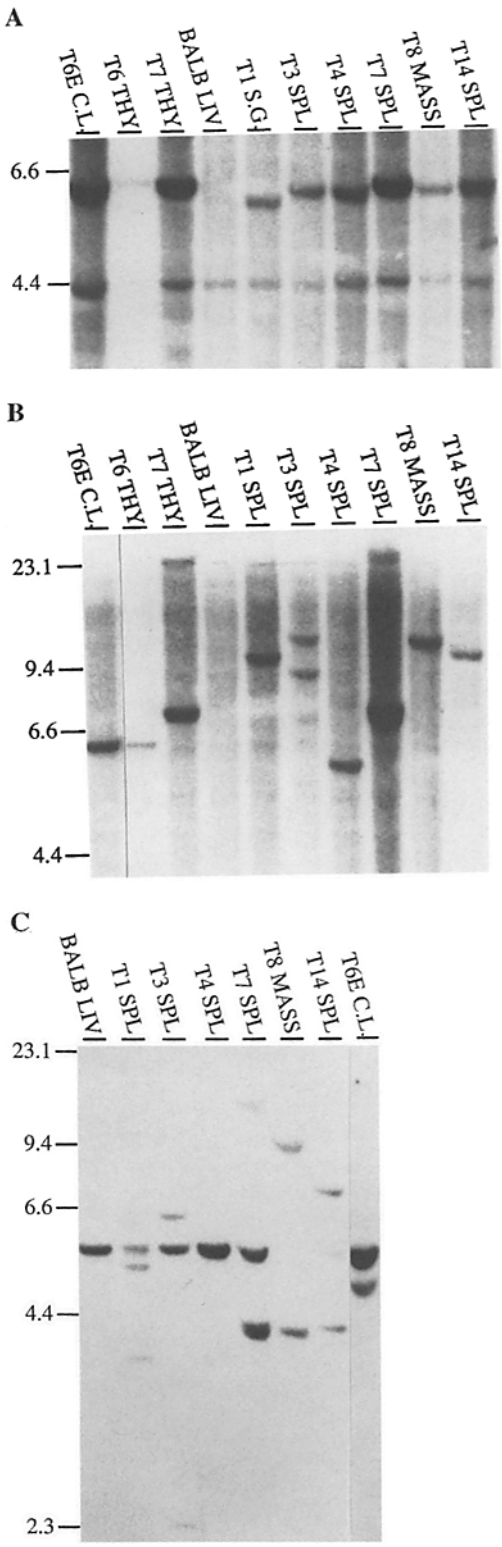

Figure 3. Analysis of *TAN1* proviral integration and TCR-β chain rearrangement in ΔECT tumors. (*A*) Southern blot of XbaI-digested genomic DNA hybridized with *TAN1* cDNA. XbaI cleaves once in each LTR (Fig. 1), generating a 6-kb fragment after hybridization to a *TAN1* probe. The 4.4-kb fragment is the endogenous *Notch1* fragment. Lanes: T6E cell line, T6 thymus, T7 thymus, BALB/c liver, T1 salivary gland, T3 spleen, T4 spleen, T7 spleen, T8 thigh mass, T14 spleen. (*B*) Southern blot of EcoRI-digested genomic DNA hybridized with *TAN1* cDNA. EcoRI cleaves once in the pGD ΔECT vectors (see Fig. 1). Lanes: T6E cell line, T6 thymus, T7 thymus, BALB/c liver, T1 spleen, T3 spleen, T4 spleen, T7 spleen, T8 thigh mass, T14 spleen. The *TAN1* hybridization probe in both *A* and *B* was a 561-bp fragment that was derived by PCR from a region of the cDNA 3′ of the ankyrin repeats (base pairs 6832–7393). (*C*) TCR β rearrangement in ΔECT tumors. DNA was digested with HindIII. The hybridization probe is the 2.2-kb EcoRI TCR-Jβ2-specific DNA fragment (37) that hybridizes to a 5-kb HindIII fragment in unrearranged DNA. Lanes: BALB/c liver, T1 spleen, T3 spleen, T4 spleen, T7 spleen, T8 thigh mass, T14 spleen, T6E cell line. 5–10 μg of DNA was loaded in each lane except T6 thymus, where 2 μg was loaded. Size markers, in kilobases, are to the left.

try performed on these tissue sections showed a high level of TAN1 expression in tumor cells relative to levels in surrounding normal tissue (Fig. 6 *b*, and data not shown). Subcellular localization of TAN1 was further investigated in disaggregated tumor and cell lines. Tumors induced with either ΔECT construct showed prominent cytoplasmic staining with TAN1-specific antibodies (Fig. 6 *c*, and data not shown). This staining colocalized with that observed using antibodies against calnexin, a protein previously shown to localize to the endoplasmic reticulum (20). This suggests that most ΔECT-produced TAN1 is present in the endoplasmic reticulum and contiguous portions of the nuclear membrane. In contrast, tumors induced by the ICT construct showed strong nuclear staining (Fig. 6 *d*, and data not shown).

Discussion

These studies show that truncated forms of TAN1 can induce T cell tumors in mice, strongly suggesting that *Notch* homologues can function as human oncogenes. Two findings support a direct role for truncated TAN1 in the pathogenesis of the murine T cell neoplasms. First, high level expression of the proteins encoded by retrovirally transmitted *TAN1* cDNAs occurred in all analyzable tumors. Second, a single integrated provirus was detected in most of the tumors, which were readily passaged in syngeneic recipients.

The current data, together with our previous experience using the bone marrow transplant assay, argue against other explanations for the high frequency of T cell malignancies observed in these animals. First, insertional mutagenesis by replication-competent helper virus seems unlikely, as the MoMLV envelope gene was absent from the malignant cells (Pear, W., unpublished data). Second, activation of leukemogenic endogenous retroviruses by the marrow transfer procedure itself is quite rare. Using bone marrow infected with retroviruses that carry different oncogenic and nononcogenic cDNA inserts, we have transplanted over 200 BALB/c mice. Of these animals, which have been followed for more than 1 yr after transplant, only one has developed a T cell malignancy (Pear W., and M. Scott, unpublished data).

The T cell specificity of transformation by TAN1 is striking and probably results from the properties of the

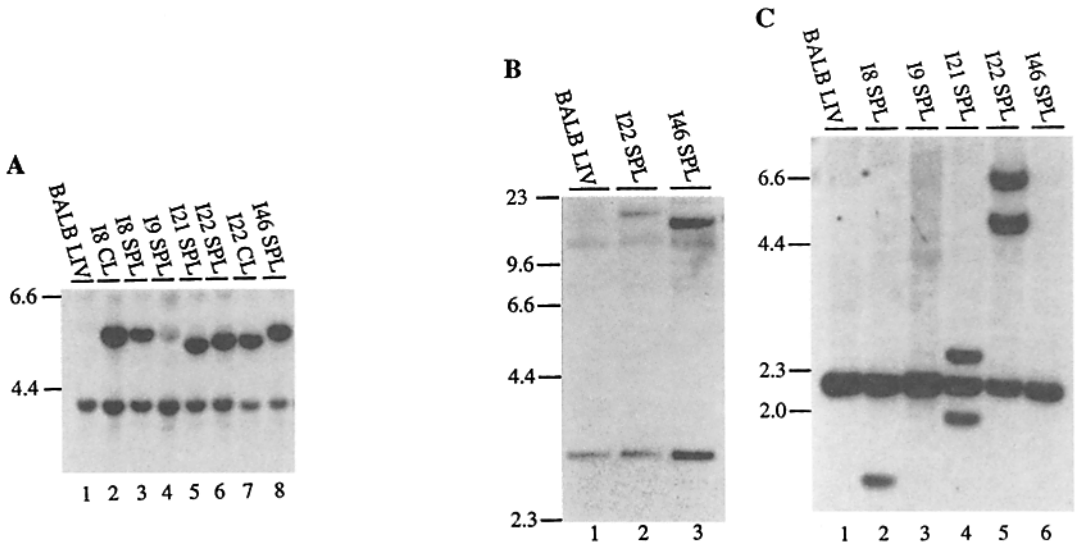

Figure 4. Analysis of *TAN1* proviral integration and TCR-β chain rearrangement in ICT tumors. (*A*) Southern blot of XbaI-digested genomic DNA hybridized with *TAN1* cDNA. XbaI cleaves once in each LTR (see Fig. 1), generating a 5.8-kb fragment after hybridization to a *TAN1* probe. The 4.4-kb fragment is the endogenous *Notch1* fragment. The smaller bands in I21 spleen (lane *5*) and I22 spleen and cell line (lanes *6* and *7*) are the result of deletions occurring outside of the *TAN1* cDNA in the integrated provirus (Fig. 1). Lanes: *1*, BALB/c liver; *2*, I8 cell line; *3*, I8 spleen; *4*, I9 spleen; *5*, I21 spleen; *6*, I22 spleen; *7*, I22 cell line; *8*, I46 spleen. (*B*) Southern blot of HindIII-digested genomic DNA hybridized with *TAN1* cDNA. HindIII cleaves outside of the pGD ICT vector. The 3-kb and ~11-kb bands are endogenous murine *Notch* sequences. Lanes: *1*, BALB/c liver; *2*, I22 spleen; *3*, I46 spleen. The *TAN1* hybridization probe in *A* and *B* was a 561-bp fragment that was derived by PCR from a region of the cDNA 3′ of the ankyrin repeats (base pairs 6832–7393). (*C*) *TCR-β* rearrangement in ICT tumors. DNA was digested with EcoRI. The hybridization probe is the 2.2-kb EcoRI *TCR-Jβ2*–specific DNA fragment (37) that hybridizes to a 2.2-kb EcoRI fragment in cells that have not undergone rearrangement of this locus. Lanes: *1*, BALB/c liver; *2*, I8 spleen; *3*, I9 spleen; *4*, I21 spleen; *5*, I22 spleen; *6*, I46 spleen. 5–10 μg of DNA was loaded in each lane. Size markers, in kilobases, are to the left.

TAN1 gene product itself and not from its route of introduction. The MoMLV LTR in the pGD vector directs high level transcription in a wide variety of hematopoietic cell types. Infection of whole bone marrow targets all dividing cells, not just T cell progenitors (21). In previous transplants using similar protocols, but different transforming genes, tumors of pre–B cell, granulocyte, macrophage, and mast cell origin occurred (9, 22–24). The T cell oncotropism of TAN1 distinguishes it from the product of *int3*, a distantly related member of the Notch family. This gene is associated with murine salivary and mammary tumors, apparently owing to the specificity of the mouse mammary tumor virus promoter, which controls transcription of the gene (25).

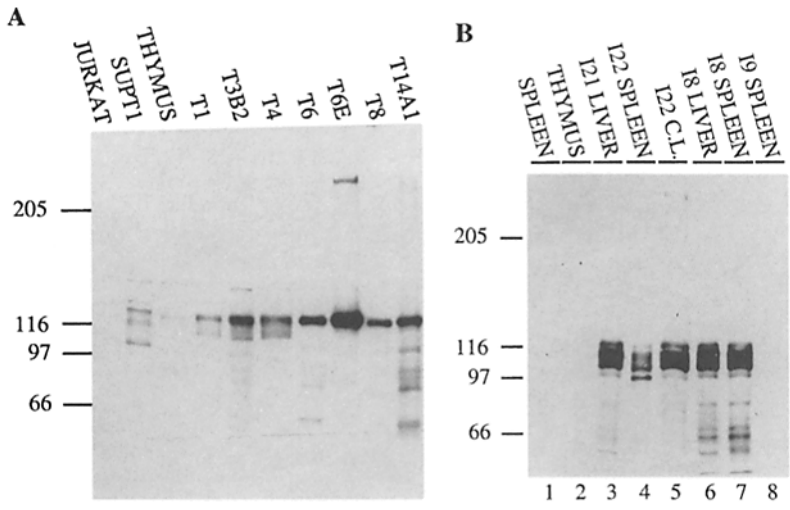

Figure 5. TAN1 protein expression in ΔECT and ICT tumors. (*A*) Western blot showing *TAN1* expression in tumors from ΔECT transplants. The ΔECT TAN1 specific product is present at ~120 kD. The band at ~350 kD in the T6E lane corresponds in size to the product of murine *Notch1* (38). A faint band in the identical position was observed in all other ΔECT tumor extracts upon longer exposure (not shown). Lanes: Jurkat, a human T-ALL with apparently normal *TAN1* alleles, SUPT1, a human T-ALL cell line with two copies of the t(7;9) and no normal *TAN1* allele, BALB/cByJ thymus, T1 spleen, T3B2 spleen (secondary transplant recipient of cells from T3 spleen), T4 spleen, T6 thymus, T6E cell line, T8 thigh mass, T14A1 spleen (secondary transplant recipient of cells from T14 spleen). (*B*) Western blot showing TAN1 expression in tumors from ICT transplants. The ICT TAN1 specific product is present at ~110 kD. A similar band was present in I46 spleen (Aster, J., unpublished data). The ~110-kD band was not detectable in I9 spleen owing to the small amount of tumor present in the liver and spleen of this animal. The band at ~350 kD in the I22 cell line (lane *5*) corresponds in size to the product of murine *Notch1* (38). A faint band in the identical position was observed in all other ICT tumor extracts upon longer exposure. The ~120-kD TAN1-specific band corresponding to the proteolytic cleavage product is present in BALB/c thymus upon longer exposure. Lanes: *1*, BALB/c spleen; *2*, BALB/c thymus; *3*, I21 liver; *4*, I22 spleen; *5*, I22 cell line; *6*, I8 liver; 7, I8 spleen; *8*, I9, spleen. 10 μg of protein was loaded in each lane. The size markers, in kD, are to the left.

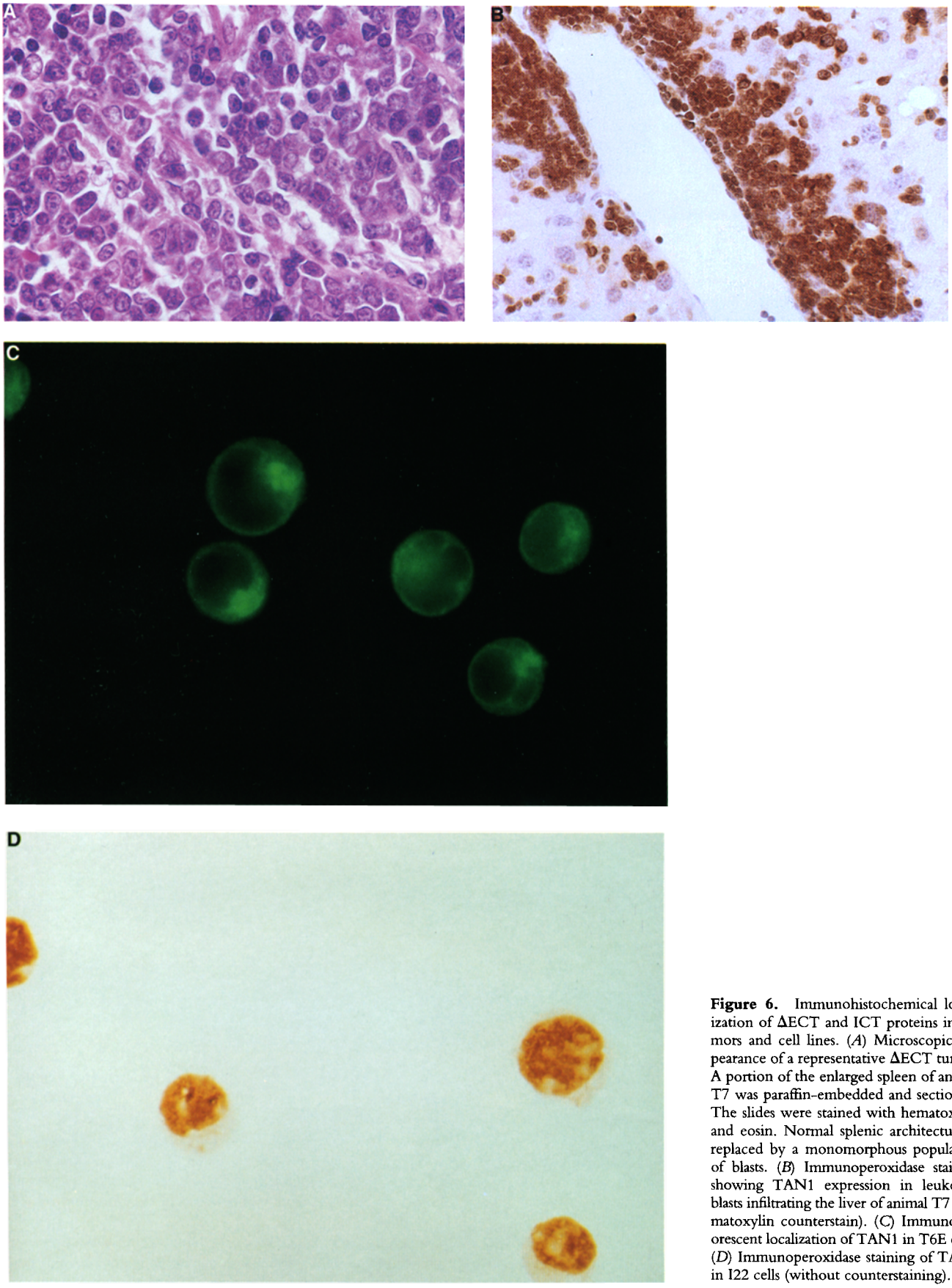

Figure 6. Immunohistochemical localization of ΔECT and ICT proteins in tumors and cell lines. (*A*) Microscopic appearance of a representative ΔECT tumor. A portion of the enlarged spleen of animal T7 was paraffin-embedded and sectioned. The slides were stained with hematoxylin and eosin. Normal splenic architecture is replaced by a monomorphous population of blasts. (*B*) Immunoperoxidase staining showing TAN1 expression in leukemic blasts infiltrating the liver of animal T7 (hematoxylin counterstain). (*C*) Immunofluorescent localization of TAN1 in T6E cells. (*D*) Immunoperoxidase staining of TAN1 in I22 cells (without counterstaining).

Unlike several other genes implicated in the pathogenesis of T-ALL, including *TAL1, RBTN2,* and *HOX11,* which are not normally expressed in thymocytes (26–29), *Notch1/TAN1* is expressed at high levels in normal thymus (1) and is also expressed in $CD34^+$ stem cells within the bone marrow (30). The highest levels of TAN1 expression in murine and human thymus occur in cortical thymocytes (3a), and all of the TAN1-associated tumors described in this report have immunophenotypes resembling those of normal cortical thymocytes. The normal function of *TAN1* in T cells and marrow progenitor cells is unknown. However, recent developmental studies in flies, frogs, and cultured murine cells have shown that truncated forms of Notch-related proteins inhibit certain programs of differentiation (2). For example, truncated Notch1 inhibits neurogenesis and myogenesis of murine embryonal carcinoma cells (31, 32). These and other observations support the idea that Notch expression maintains various cell types in a less differentiated state (3, 33). Our studies suggest that truncated TAN1 might act in a similar fashion within T cell progenitors by preventing their terminal differentiation and predisposing them to malignant transformation.

The apparent ability of truncated TAN1 to transform regardless of subcellular localization is puzzling. Although it is possible that a small amount of nuclear protein in the ΔECT tumors is responsible for transforming activity (or that a small amount of cytoplasmic protein is culpable in ICT tumors), it is noteworthy that functional equivalence of cytoplasmic and nuclear forms of truncated Notch has also been observed in a number of other systems, particularly those assessing effects on eye, wing, and bristle development in the fly (7, 8). ΔECT-like polypeptides also perturb myogenesis and neurogenesis in developing frogs (34). One possible explanation for the functional equivalence of cytoplasmic and nuclear Notch proteins would involve interaction with downstream factors that normally shuttle between the nucleus and the cytoplasm. Candidate proteins include several transcription factors that are believed to interact with Notch on on the basis of genetic data (2). The subcellular localization of one molecule, Suppressor of Hairless (Su(H)), appears to be controlled by activation of Notch through binding of ligand to the extracellular domain. This suggests that Su(H) participates in Notch signaling in some cell types in the fly (35). A mammalian homologue of Su(H), CBF1 (also known as RBP-J kappa), has been shown to activate transcription following interaction with murine Notch1 (36). Preliminary results show that Su(H) interacts with both the ΔECT and ICT proteins (Aster, J., unpublished data), suggesting that this molecule is involved in neoplastic signaling in these tumors. Elucidation of this signalling pathway and the activated genes awaits further analysis.

We thank Dr. C. Guidos and members of the Baltimore and Sklar laboratories for helpful discussions. We also thank Dr. G. Pinkus for help with immunohistochemistry, and V. Patriuvavicius for technical assistance. We gratefully acknowledge Dr. K. LaMarco and Dr. W. Sha for critical reading of the manuscript.

W.S. Pear was supported by a Physician Postdoctoral Fellowship from the Howard Hughes Medical Institute and is presently a Special Fellow of the Leukemia Society of America. J.C. Aster is supported by a Research Grant from the Massachusetts Division of the American Cancer Society. R.P. Hasserjian is supported by National Institutes of Health training grant number 5T32HL-07627. This work was supported by National Institutes of Health grant number CA-38621 to J.Sklar and 7R37AI-2234613 to D. Baltimore.

Address correspondence to Dr. David Baltimore, Massachusetts Institute of Technology, Room 68-380, 77 Massachusetts Avenue, Cambridge, MA 02139-4307.

Received for publication 5 January 1996.

References

1. Ellison, L.W., J. Bird, D.C. West, A.L. Soreng, T.C. Reynolds, S.D. Smith, and J. Sklar. 1991. TAN-1, the human homologue of the Drosophila *Notch* gene, is broken by chromosomal translocations in T lymphoblastic neoplasms. *Cell.* 66: 649–661.
2. Artavanis-Tsakonas, S., K. Matsuno, and M.E. Fortini. 1995. Notch signaling. *Science (Wash. DC).* 2688:225–232.
3. Greenwald, I. 1994. Structure/function studies of lin-12/Notch proteins. *Curr. Opin. Genet. Dev.* 4:556–562.
3a. Hasserjian, R.H., J.C. Aster, F. Davi, D. Weinberg, and J. Sklar. 1996. Modulated expression of Notch 1 during development. *Blood.* In press.
4. Reynolds, T.C., S.D. Smith, and J. Sklar. 1987. Analysis of DNA surrounding the breakpoints of chromosomal translocations involving the β T cell receptor gene in lymphoblastic neoplasms. *Cell.* 50:107–117.
5. Smith, S.D., R. Morgan, R. Gemmell, M.D. Amylon, M.P. Link, C. Linker, B.K. Hecht, R. Warnke, B.E. Glader, and F. Hecht. 1988. Clinical and biologic characterization of T-cell neoplasias with rearrangements of chromosome 7 band q34. *Blood.* 71:395–402.
6. Struhl, G., K. Fitzgerald, and I. Greenwald. 1993. Intrinsic activity of the lin-12 and notch intracellular domains in vivo. *Cell.* 74:331–345.

7. Rebay, I., R.G. Fehon, and S. Artavanis-Tsakonas. 1993. Specific truncations of Drosophila Notch define dominant activated and dominant negative forms of the receptor. *Cell.* 74:319–329.
8. Lieber, T., S. Kidd, E. Alcamo, V. Corbin, and M.W. Young. 1993. Antineurogenic phenotypes induced by truncated Notch proteins indicate a role in signal transduction and may point to a novel function for Notch in nuclei. *Genes Dev.* 7:1949–1965.
9. Daley, G.Q., R.A. Van Etten, and D. Baltimore. 1990. Induction of chronic myelogenous leukemia in mice by the P210 *bcr/abl* gene of the Philadelphia chromosome. *Science (Wash. DC).* 247:824–830.
10. Pear, W., G. Nolan, M. Scott, and D. Baltimore. 1993. Production of high-titer helper-free retroviruses by transient transfection. *Proc. Natl. Acad. Sci. USA.* 90:8392–8396.
11. Ausubel, F.M., R. Brent, R.E. Kingston, D.D. Moore, J.G. Seidman, J.A. Smith, and K. Struhl. 1989. Current protocols in Molecular Biology. John Wiley & Sons, Inc., New York.
12. Shan-Rong, S., B. Chaiwun, L. Young, R.J. Cote, and C.R. Taylor. 1993. Antigen retrieval technique utilizing citrate buffer of urea solution for immunohistochemical demonstration of androgen receptor in formalin-fixed paraffin sections. *J. Histochem. Cytochem.* 41:1599–1604.
13. Pinkus, G.S., E.M. O'Connor, C.L. Etheridge, and J.M. Corson. 1985. Optimal immunoreactivity of keratin proteins in formalin-fixed, paraffin-embedded tissue requires preliminary trypsinization. An immunoperoxidase study of various tumors using polyclonal and monoclonal antibodies. *J. Histochem. Cytochem.* 33:465–473.
14. Coligan, J.E., A.M. Kruisbeek, D.H. Margulies, E.M. Shevach, and W. Strober. 1992. Current Protocols in Immunology. John Wiley & Sons, New York.
15. Paterson, D.J., and A.F. Williams. 1987. An intermediate cell in thymocyte differentiation that expresses CD8 but not CD4 antigen. *J. Exp. Med.* 166:1603–1608.
16. MacDonald, H.R., R.C. Budd, and R.C. Howe. 1988. A $CD3^-$ subset of $CD4^-$ $CD8^+$ thymocytes: a rapidly cycling intermediate in the generation of $CD4^+$ $CD8^+$ cells. *Eur. J. Immunol.* 18:519–523.
17. Guidos, C.J., I.L. Weissman, and B. Adkins. 1989. Intrathymic maturation of murine T lymphocytes from $CD8^+$ precursors. *Proc. Natl. Acad. Sci. USA.* 86:7542–7546.
18. Turka, L.A., D.G. Schatz, M.A. Oettinger, J.M. Chun, C. Gorka, K. Lee, W.T. McCormack, and C.B. Thompson. 1991. Thymocyte expression of RAG-1 and RAG-2: termination by T cell receptor cross-linking. *Science (Wash. DC).* 253:778–781.
19. Zagouras, P., S. Stefano, C.M. Blaumueller, M.L. Carcangiu, and S. Artavanis-Tsakonas. 1995. Alterations in Notch signaling in neoplastic lesions of the human cervix. *Proc. Natl. Acad. Sci. USA.* 92:6414–6418.
20. Hochstenbach, F., V. David, S. Watkins, and M.B. Brenner. 1992. Endoplasmic reticulum resident protein of 90 kilodaltons associates with the T- and B-cell antigen receptors and major histocompatibility complex antigens during their assembly. *Proc. Natl. Acad. Sci. USA.* 89:4734–4738.
21. Keller, G., C. Paige, E. Gilboa, and E.F. Wagner. 1985. Expression of a foreign gene in myeloid and lymphoid cells derived from multipotent hematopoietic precursors. *Nature (Lond.).* 318:149–154.
22. Scott, M.L., R.A. Van Etten, G.Q. Daley, and D. Baltimore. 1991. v-*abl* causes hematopoietic disease distinct from that caused by *bcr-abl. Proc. Natl. Acad. Sci. USA.* 88:6506–6510.
23. Kamps, M.P., and D. Baltimore. 1993. E2A-Pbx1, the t(1; 19) translocation protein of human pre–B-cell acute lymphocytic leukemia, causes acute myeloid leukemia in mice. *Mol. Cell. Biol.* 13:351–357.
24. Gurish, M.F., W.S. Pear, R.L. Stevens, M.L. Scott, K. Sokol, N. Ghildyal, M.J. Webster, X. Hu, K.F. Austen, D. Baltimore, and D.S. Friend. 1995. Tissue-regulated differentiation and maturation of a v-*abl*-immortalized mast cell–committed progenitor. *Immunity.* 3:175–186.
25. Jhappan, C., D. Gallahan, C. Stahle, E. Chu, G.H. Smith, G. Merlino, and R. Callahan. 1992. Expression of an activated Notch-related *int-3* transgene interferes with cell differentiation and induces neoplastic transformation in mammary and salivary glands, *Genes Dev.* 6:345–355.
26. Chen, Q., J.T. Cheng, L.H. Tasi, N. Schneider, G. Buchanan, A. Carroll, W. Crist, B. Ozanne, M.J. Siciliano, and R. Baer. 1990. The *tal* gene undergoes chromosome translocation in T cell leukemia and potentially encodes a helix-loop-helix protein. *EMBO Eur. Mol. Biol. Org. J.* 9:415–424.
27. Hatano, M., C.W. Roberts, M. Minden, W.M. Crist, and S.J. Korsmeyer. 1991. Deregulation of a homeobox gene, *HOX11*, by the t(10;14) in T cell leukemia. *Science (Wash. DC).* 253:79–82.
28. Dube, I.D., R.S. Kamel, C.C. Yuan, M. Lu, X. Wu, G. Corpus, S.C. Raimondi, W.M. Crist, A.J. Carroll, J. Minowada, et al. 1991. A novel human homeobox gene lies at the chromosome 10 breakpoint in lymphoid neoplasias with chromosomal translocation t(10;14). *Blood.* 78:2996–3003.
29. Rabbitts, T.H. 1994. Chromosomal translocations in human cancer. *Nature (Lond.).* 372:143–149.
30. Milner, L.A., R. Kopan, D.I. Martin, and I.D. Bernstein. 1994. A human homologue of the Drosophila developmental gene, *Notch*, is expressed in $CD34^+$ hematopoietic precursors. *Blood.* 83:2057–2062.
31. Kopan, R., J. Nye, and H. Weintraub. 1994. The intracellular domain of mouse Notch: a constitutively activated repressor of myogenesis directed at the basic helix-loop-helix region of MyoD. *Development.* 120:2385–2396.
32. Nye, J., R. Kopan, and R. Axel. 1994. An activated Notch suppresses neurogenesis and myogenesis but not gliogenesis in mammalian cells. *Development.* 120:2421–2430.
33. Fortini, M.E., and S. Artavanis-Tsakonas. 1994. The Suppressor of Hairless protein participates in notch receptor signaling. *Cell.* 79:259–272.
34. Coffman, C.R., P. Skogland, W.A. Harris, and C.R. Kintner. 1993. Expression of an extracellular deletion of Xotch diverts cell fate in Xenopus embryos. *Cell.* 73:659–671.
35. Fortini, M.E., and S. Artavanis-Tsakonas. 1994. Notch: neurogenesis is only part of the picture. *Cell.* 75:1245–1247.
36. Jarriault, S., C. Brou, F. Logeat, E.H. Schroeter, R. Kopan, and A. Israel. 1995. Signalling downstream of activated mammalian Notch. *Nature (Lond.).* 377:355–358.
37. Fenton, R.G., P. Marrack, J.W. Kappler, O. Kanagawa, and J.G. Seidman. 1988. Isotypic exclusion of γ δ T cell receptors in transgenic mice bearing a rearranged β-chain gene. *Science (Wash. DC).* 241:1089–1092.
38. Reaume, A.G., R.A. Conlon, R. Zirngibl, T.P. Yamaguchi, and J. Rossant. 1992. Expression analysis of a Notch homologue in the mouse embryo. *Dev. Biol.* 154:377–387.